Numerical Demonstration of THz Traveling Wave Amplifications in 2-D Electron Gas (2DEG) Under Scattering-Free and Low-Charge Density Regime

Shubhendu Bhardwaj[®], Member, IEEE, and Md Faiyaz Bin Hassan[®]

Abstract-In this letter, we investigate the terahertz field fluctuations and dynamic interactions with electrons in a 2-D electron gas (2DEG) under the influence of slow wave structure in a substrate-based device. Low-charge density and the scattering-free regime are considered to maintain practical simulation times. The dynamics of this interaction are simulated using a co-planar waveguide (CPW)-connected interdigitated metal grating structure to provide electromagnetic (EM) excitation and phase velocity comparable to electron drift in the 2DEG channel. This letter demonstrates that interdigitated slow wave structure provides a media for synchronous interaction between electron gas and EM waves leading to amplification of charge density and velocity oscillations in a 2DEG. The method used for this numerical work is a full-wave-global numerical model that uses finite-difference time domain (FDTD)-based particle in cell solver of electron transport in 2DEG, with self-consistent EM field solution. Under the considered regime and device, the current oscillations show an increase in amplitude which illustrates the effect of synchronous interaction between the 2DEG.

Index Terms—2-D electron gas (2DEG), amplifier, high electron mobility transistors (HEMTs), terahertz, traveling wave gain.

I. INTRODUCTION

TRAVELING wave gain occurs due to synchronous interactions between electrons traveling at a finite velocity and electromagnetic (EM) wave subject to a slow wave effect [1], [2]. Specifically, under the condition of electron drift velocity (v_d) being approximately equal to the phase velocity (v_p) of the surrounding EM wave, $(v_p = v_d)$, gain in the wave's amplitude is anticipated. Sub-mm-wave and terahertz monolithic microwave amplifiers have the potential to replicate this phenomenon within substrates compatible with monolithic microwave integrated circuits (MMICs) [3], [4]. In this configuration of amplifier device, a slow wave structure based on interdigitated fingers is shown to be useful [5], [6], while 2-D electron gas (2DEG) implementation based on high electron mobility transistors (HEMTs) [7] or 2-D materials [8] has been suggested.

Manuscript received 28 February 2024; revised 21 March 2024; accepted 27 March 2024. Date of publication 16 April 2024; date of current version 7 June 2024. This research was supported by award no. 2329940 from National Science Foundation, titled "Semiconductor-based Terahertz Traveling Wave Amplifiers for Monolithic Integration". (Corresponding author: Shubhendu Bhardwaj.)

The authors are with the Electrical and Computer Engineering, University of Nebraska-Lincoln, Lincoln, NE 68588 USA (e-mail: bhardwaj@unl.edu). This article was presented at the IEEE MTT-S International Microwave

Symposium (IMS 2024), Washington, DC, USA, June 16–21, 2024. Color versions of one or more figures in this letter are available at https://doi.org/10.1109/LMWT.2024.3383769.

Digital Object Identifier 10.1109/LMWT.2024.3383769

Numerical modeling is critical for device's physical understanding and predicting its performance. For this purpose, full-wave-global models [9] need to be adopted with the condition that electron transport is modeled using a particle-based approach such as ensemble Monte Carlo (EMC). Therefore, numerical modeling poses a computational challenge, especially because the bulk carrier or velocity approximations (such as by using a hydrodynamic model) often used to reduce modeling computation time are not accurate here [10]. While using particle solution, grid sizes are sub-one-thousandth of the wavelength near 2DEG, and the simultaneous solution of Maxwell's equation is a computational challenge. The use of commercial particle-in-cell (PIC) solvers can be considered; however, the use of 3-D models, high charge densities, and time-domain limitations of Courant-Friedrichs-Lewy (CFL) condition [11], such solvers remain slow for our applications.

In this letter, we present the numerical modeling results, where 2DEG of a high HEMT or other 2-D materials interact with an interdigitated slow wave structure [see Fig. 1(a)]. Due to the computational cost of this multiscale simulation, we limit the carrier density to $n_{\rm sh}=10^8~{\rm cm}^{-2}$ for a reasonable simulation time (\approx 5–7 days). Smaller charge density is chosen to allow mesh sizes that are solvable for this problem, and negligible scattering could be a reasonable approximation for some 2DEG systems such as low-temperature graphene. Under this regime, gain in the ac current oscillations is observed in the 2DEG at 300 GHz. The device model, simulation method, and results are discussed in this letter.

II. SIMULATED STRUCTURE AND EXCITATION MODEL

A. Device Model

The device under investigation is shown in Fig. 1(a) and (b). The configuration of the device consists of a substrate upon a heterogeneous or substrate stack (such as GaAs/AlGaAs, GaN/AlGaN, or h-BN for graphene). The goal of the simulation is to model EM interactions between the slow wave structure and the underlying 2DEG electrons; therefore, the simulations should be instructive for different material systems. An Au-interdigitated electrode connected to signal and ground lines on either side of a co-planar waveguide (CPW) line is used as a slow wave structure. The structure acts as a floating metallic gate positioned at a vertical barrier distance of $d_{\text{barr}} = 10$ nm from the 2DEG. Drain and source terminals are connected with the 2DEG but are isolated from the slow wave structure.

The grating periodicity plays an important role in synchronizing the antimodal fields in the grating region with the electron drift velocity. The excitation frequency was chosen

2771-957X © 2024 IEEE. Personal use is permitted, but republication/redistribution requires IEEE permission. See https://www.ieee.org/publications/rights/index.html for more information.

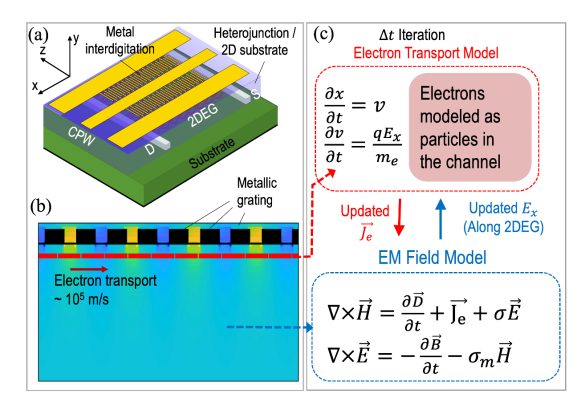


Fig. 1. (a) Device configuration for feeding and implementing the slow wave in the vicinity of a 2DEG structure. (b) Cross section of the configuration. (c) Equations involved in the solution of electron transport and EM fields.

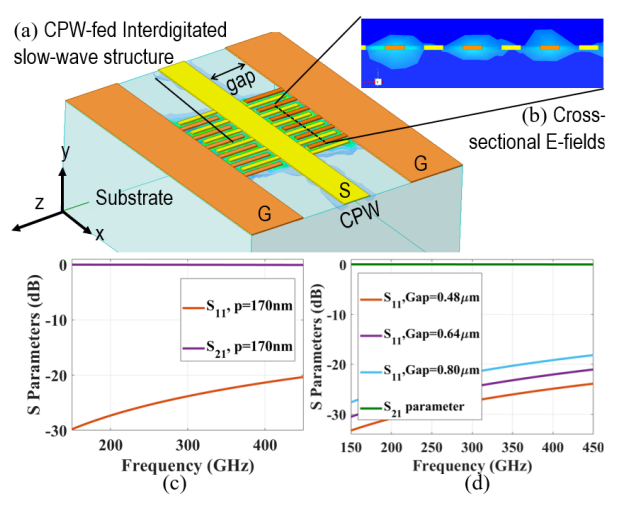
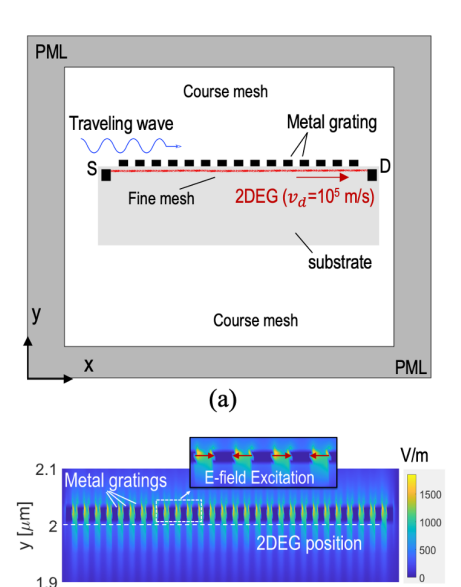


Fig. 2. Passive tests of the device showing (a) 3-D model used, (b) *E*-field observed near the interdigitations, (c) S_{11} and S_{21} for p=170 nm, and (d) effect of gap variation.

to be at a lower terahertz band of 300 GHz. The general rule of design based on the Pierce theory of synchronous operation should satisfy $v_d = f \times 2p$. Therefore, for f = 300 GHz, and $v_d = 10^5$ m/s, grating periodicity $p \approx 166$ nm is chosen for this simulation.

B. Excitation in the Device Model

The dc biasing of the device is considered by assuming an initial drift velocity of carriers (electrons) at $v_d = 10^5$ m/s in the 2DEG channel by applying sufficient bias at the drain (D) and source (S) terminals of the device. This choice of drift velocity is consistent with the achievable drift velocity in the channel in most material systems. For RF excitation, the model requires feeding of RF signal at 300 GHz through CPW lines. A multiphysics modeling of the entire 3-D structure which includes CPW lines and device stack is computationally expensive; therefore, a reduced 2-D cross-sectional model focused on the grating region was used. Although in the 3-D model, the excitation is provided through CPW lines (Fig. 2), this excitation translates to a field profile used in Fig. 3(b). Therefore, this field profile can be mimicked by using lumped sources introduced in the 2-D model applied between the metal gratings, such that a reversed polarity between the neighboring gaps is exhibited. This choice of electric field is confirmed by observing the fields in the cross section of the interdigitated metal grating through a finite-element method-based single physics solver [Fig. 2(b)].



(b)Fig. 3. (a) Simulation domain of the 2-D cross section of the device. (b) Field excitation in the grating region. The total E-field $|(E_x^2 + E_y^2)^{1/2}|$ are plotted

III. FINITE-DIFFERENCE TIME DOMAIN (FDTD)–EMC GLOBAL MODEL AND ASSUMPTIONS FOR ANALYSIS

A. Full-Wave Passive Device Modeling

To understand the passive performance of interdigitated CPW structure, passive (cold) full-wave simulations were conducted at 300 GHz (with p=170 nm and a selection of gap). In Fig. 2(a) and (b), we show electric field distribution observed in a reduced length version of slow wave structure in vertical (xy plane). As shown in Fig. 2(c), S_{11} between -30 and -20 dB and S_{21} close to 0 dB is found around 300 GHz for a full-length device. CPW gap which has significance for the area of the device was varied to investigate its impact and is plotted in Fig. 2(d). These simulations serve to validate the performance of the slow wave structure and its field profile though cold test simulations.

B. FDTD-EMC Modeling of Traveling Wave Phenomenology

Using the excitation method identified Section II-B, a TE_z solution of EM waves can be pursued to model the device's cross section located in the xy plane. Fig. 3(a) shows the not-to-scale model, where the numerical solution of Maxwell's equations is pursued

$$\nabla \times \vec{H} = \frac{\partial \vec{D}}{\partial t} + \vec{J}_e \text{ (Ampere's law)} \tag{1}$$

$$\nabla \times \vec{E} = -\frac{\partial \vec{B}}{\partial t} \text{ (Faraday's law)} \tag{2}$$

where variables \vec{E} , \vec{D} , \vec{H} , and \vec{B} carry their usual meaning related to electric and magnetic fields, while \vec{J}_e is the ac component of the electric current due to electron's motion in the channel. A PIC solver is used to model the motion of electrons in a single dimension through the following equations:

$$\frac{\partial v_i}{\partial t} = -\frac{E_x q_e}{m_e} \text{ and } \frac{\partial x_i}{\partial t} = v_i$$
 (3)

where individual particle's position (x_i) and velocity (v_i) are calculated at each time step under the influence of the electric field's x-component E_x along the channel. Here, q_e is the charge on one electron and m_e is the effective mass of the electron in the 2DEG. By using the velocity of all the particles in a cell, aggregate velocity times the number of electrons per unit length is calculated as sheet density (j_{sh}) , which can then be used to calculate the current density $\vec{J}_e = \hat{x} J_e$ in the channel

$$J_e = \frac{q_e j_{\rm sh}}{t_{\rm 2DEG}} \tag{4}$$

where $t_{\rm 2DEG}$ is the thickness of the 2DEG channel. The current obtained here can be fed back into Ampere's law (1) at the end of each time iteration to evaluate the EM fields in the next time iteration. By repeating this iteration $T_{\rm total}/\Delta t_{\rm FDTD}$ times, the simulation is thus completed by reaching a point of nontransient or stable oscillation. Here, $T_{\rm total}$ is the total simulation time, and $\Delta t_{\rm FDTD}$ is the FDTD time step.

C. Multiscale Meshing and Allowable Maximum Time Step

To maintain the stability of a time-domain simulation, the maximum value of time-step ($\Delta t_{\rm FDTD}$) should be chosen within the Courant limit for maximum time step [11]. For multiphysics electronic–EM simulation, this limit is subjected to much finer mesh size, i.e., Δx and $\Delta y \approx \lambda/10\,000$. This small grid size is associated with the stability of the ensemble MC simulation which could become unstable if the mesh size is not comparable or a fraction of the Debye length of the electron gas. In such a case the feedback loop between the electron transport and EM solver could become unstable leading to simulation divergence.

To minimize the simulation time for the proposed device, we use adaptive mesh in the regions of the device. As shown in Fig. 3(a), an adaptive mesh is chosen in the cross section, which reduces the total number of grid points in the simulation.

Considering the limited computational resources, we study the device's current gain phenomenology in the regime of low sheet carrier density $n_{\rm sh}=10^8~{\rm cm}^{-2}$. At such low levels of $n_{\rm sh}$, the Debye length is approximately 370 nm ($\lambda_D=(KT\epsilon_o\epsilon_r/n_{3D}q_e^2)^{1/2}$) which allows the choice of mesh size for x- and y-directions to be $\Delta x=\Delta y=10$ nm. For this calculation, we have chosen $\epsilon_r=9.5$ for the GaN/AlGaN HEMT environment. Another simplification made in this modeling is lack of scattering in the channel, which in practice could limit the possible amplification in the channel. Nonetheless, under these simplified assumptions, the simulation is aimed at shedding light into critical functional questions of this device concept, such as the possibility of gain under given barrier dimensions, the effectiveness of the interdigitated fingers as slow wave structure, and possible limits of gain of ac amplitude.

IV. SIMULATION RESULTS

The phenomenology of traveling wave for a device of channel length $L=5~\mu m$, where the simulation was initialized with electrons drifting with velocity $v_d=10^5$ m/s. To excite the traveling wave, RF amplitude of $E_x=10^4$ V/m was used between the gratings. We have chosen $\epsilon_r=9.5$ for GaN/AlGaN HEMT environment for 2DEG to model oscillations. As noted before f=300 GHz, periodicity p=170 nm is chosen. Under these conditions, the time step for the simulation was $\Delta t_{\rm FDTD}=1.18\times 10^{-17}$ s and to complete the

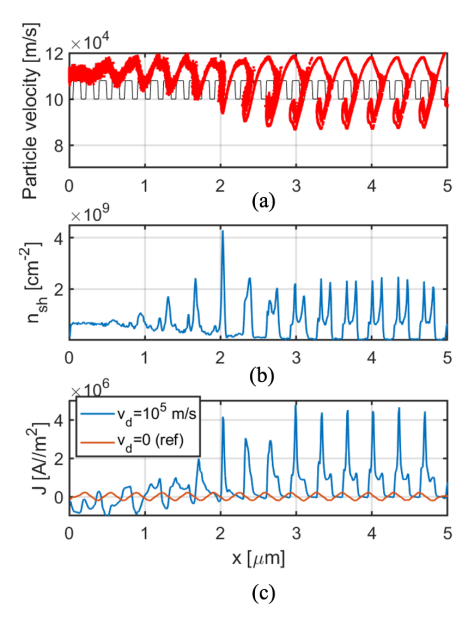


Fig. 4. (a) Carrier velocity distribution of electrons along the channel. (b) Calculated carrier density. (c) Current density J_{ℓ} along the channel.

total simulation time $T_{\text{total}} = 28$ ps using a MATLAB code, 2.3M iteration were run which concluded in approximately 5 days.

A. Modulation of Velocity, Electron Sheet Density, and Current

To measure the interaction between the EM wave and electrons in channel, we plot the scatter plot of the particles in the 2DEG, as shown in Fig. 4(a), sheet carrier density $n_{\rm sh}$ along the length in Fig. 4(b) and ac current J_e along the length of the channel Fig. 4(c). In Fig. 4(a), we note that velocity modulation of the particles is observed with a periodicity of 2p, which is consistent with the excitation. Moreover, the amplitude of the modulations increases along the length of the channel between x = 0 and $x = 3 \mu m$. This section of the 2DEG shows an amplification in the velocity modulations under a positive feedback of the EM fields, which is synchronous with the particle velocity. In other words, the particles cross through a distance of one periodicity in a time period producing a constructive addition of amplitude and amplification. However this effect saturates at $x = 3 \mu m$, and we observe uniform oscillations in the region $x > 5 \mu m$. This is due to a nonlinear effect caused by an over modulation of the electron velocity. We note that the amplitude of velocity oscillations is approximately 30% of v_d , which is typical of based slow wave devices.

Due to the modulation of the velocity of electrons, we also note accumulation of carriers at the two edges of grating in each period [see Fig. 4(b)]. This is due to the acceleration and deceleration of electrons in periodic regions of the channel, causing grouping of electrons and progressive amplification along the length of the 2DEG.

B. Discussion and Interpretation of Amplification

In Fig. 4(c), we plot the current density which is representative of the product of quantities in Fig. 4(a) and (b). A case with zero traveling wave gain (due to no bias or $v_d = 0$) is also plotted which represents the reference case for comparison of amplification. In this case, due to no applied dc drift in electrons, the positive feedback and amplification effect is not possible. A comparison between the peak-to-peak currents in

the two scenarios shows an amplification of 10.5 times in the current density for $x > 3 \mu m$.

The model simulation shows that an interdigitated structure which creates an alternating polarity grating field in the vicinity of the 2DEG can interact with 2DEG to cause spatial velocity modulations of the electron gas. This effect, indeed, is capable of creating an amplifying modulation of electron velocity, leading to density fluctuation that amplifies over the traveling distance. The simulation also shows the saturation of amplification of the oscillations, which is indicative of replication of traveling wave amplification in micrometer-long device. An analogy of this effect is already established in traveling wave vacuum tubes.

V. CONCLUSION

In this letter, we have numerically demonstrated the traveling wave phenomenology in micrometer-long devices using global full-wave models. The use of PIC algorithm for 2DEG modeling and simultaneous solution of Maxwell's equations in the vicinity are helpful in establishing the rigor of this numerical simulation. The use of lower carrier density in a full-wave global numerical model allows minimum mesh sizes to be around 10 nm, which allows the simulation to be feasible in a large simulation grid consisting of many micrometer-long channels. In essence, the simulation confirms the amplification of velocity modulations originating from a synchronous interaction with EM fields in the interdigitated metal structure. Current results also demonstrate the efficacy of the interdigitated grating which can act as a slow wave structure to reduce the phase velocity of an EM traveling wave to create reduced synchronous wave behavior in micrometerlong devices.

REFERENCES

- J. R. Pierce, "Theory of the beam-type traveling-wave tube," *Proc. IRE*, vol. 35, no. 2, pp. 111–123, Feb. 1947.
- [2] A. N. Korolev et al., "Traditional and novel vacuum electron devices," IEEE Trans. Electron Devices, vol. 48, no. 12, pp. 2929–2937, Dec. 2001.
- [3] P. Makhalov, D. Lioubtchenko, and J. Oberhammer, "Semiconductor-metal-grating slow wave amplifier for sub-THz frequency range," *IEEE Trans. Electron Devices*, vol. 66, no. 10, pp. 4413–4418, Oct. 2019.
- [4] P. Pousi, D. Lioubtchenko, S. Dudorov, and A. V. Raisanen, "Dielectric rod waveguide travelling wave amplifier based on AlGaAs/GaAs heterostructure," in *Proc. 38th Eur. Microw. Conf.*, Oct. 2008, pp. 1082–1085.
- [5] H. Baudrand, T. El Khoury, and D. Lilonga, "Amplification by interdigital excitation of space-charge waves in semiconductors," *IEEE Trans. Microw. Theory Techn.*, vol. MTT-32, no. 11, pp. 1434–1441, Nov. 1984.
- [6] A. M. Hashim, S. Kasai, T. Hashizume, and H. Hasegawa, "Integration of interdigital-gated plasma wave device for proximity communication system application," *Microelectron. J.*, vol. 38, no. 12, pp. 1263–1267, Dec. 2007
- [7] A. M. Hashim, S. Kasai, K. Iizuka, T. Hashizume, and H. Hasegawa, "Novel structure of GaAs-based interdigital-gated HEMT plasma devices for solid-state THz wave amplifier," *Microelectron. J.*, vol. 38, no. 12, pp. 1268–1272, Dec. 2007.
- [8] N. Ghafarian, H. Majedi, and S. Safavi-Naeini, "Millimetre-wave and terahertz amplification in a travelling wave graphene structure," *IEEE J. Sel. Topics Quantum Electron.*, vol. 23, no. 1, pp. 179–187, Jan. 2017.
- [9] M. A. Khorrami, S. El-Ghazaly, H. Naseem, and S.-Q. Yu, "Global modeling of active terahertz plasmonic devices," *IEEE Trans. THz Sci. Technol.*, vol. 4, no. 1, pp. 101–109, Jan. 2014.
- [10] S. Bhardwaj, "Electronic-electromagnetic multiphysics modeling for terahertz plasmonics: A review," *IEEE J. Multiscale Multiphys. Comput. Techn.*, vol. 4, pp. 307–316, 2019.
- [11] A. Taflove, S. C. Hagness, and M. Piket-May, "Computational electromagnetics: The finite-difference time-domain method," *Electr. Eng. Handbook*, vol. 3, nos. 629–670, p. 15, 2005.